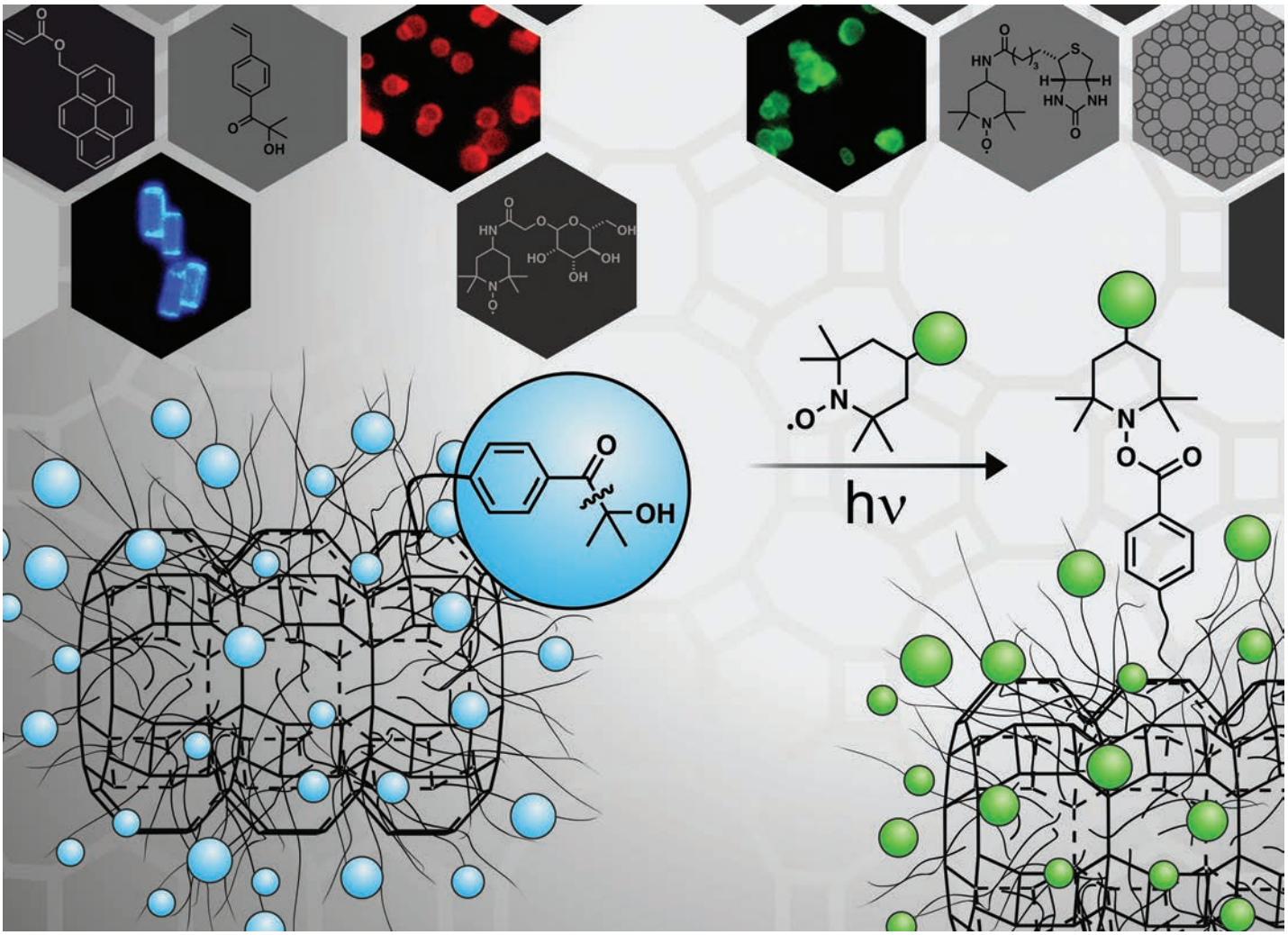

Highlighting research results from the Westfälische Wilhelms–Universität Münster, Münster, Germany.

Synthesis and photo-postmodification of zeolite L based polymer brushes

Zeolite L is a versatile material with unique properties that serves as a highly interesting building block for innovative systems. Within this work a novel type of zeolite L/polymer hybrid material is presented. Polymer brush particles are generated using surface-functionalized zeolite L crystals as macroinitiators in controlled radical polymerization processes. Copolymerization of a photo-cleavable monomer and subsequent spin trapping of functionalized nitroxides under UV irradiation leads to a variety of highly functionalized zeolite L-based core–shell particles in a modular approach.

As featured in:

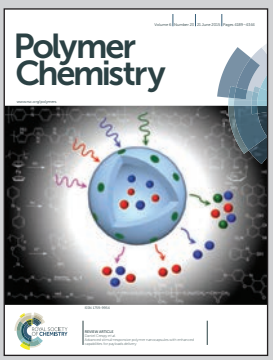

See Cornelia Denz, Armido Studer *et al.* *Polym. Chem.*, 2015, **6**, 4221.

ROYAL SOCIETY OF CHEMISTRY

www.rsc.org/polymers

Registered charity number: 207890

Polymer Chemistry

PAPER

View Article Online
View Journal | View Issue

Cite this: *Polym. Chem.*, 2015, **6**, 4221

Synthesis and photo-postmodification of zeolite L based polymer brushes†

Tim Buscher,[a] Álvaro Barroso,[b] Cornelia Denz*[b] and Armido Studer*[a]

Received 23rd March 2015,
Accepted 28th April 2015

DOI: 10.1039/c5py00425j

www.rsc.org/polymers

A novel type of zeolite L/polymer hybrid material is presented. Polymer brush particles are generated using surface-functionalized zeolite L crystals as macroinitiators in controlled radical polymerization processes. Copolymerization of a photo-cleavable monomer and subsequent spin trapping of functionalized nitroxides under UV irradiation lead to a variety of highly functionalized zeolite L based core–shell particles.

Introduction

The mineralogical group of zeolites comprises all hydrated aluminosilicates with over 200 natural and artificial modifications.[1] Zeolites are industrially used in heterogeneous catalysis and are also well known as ion exchange materials.[2] Synthetic zeolite Linde Type L (LTL, zeolite L) crystals are solid, optically transparent and physiologically stable nanocontainers with a size range from 30 nm up to 10 μm. The microporous structure of zeolite L is unique for its hexagonally arranged one-dimensional strictly parallel pores (0.76–1.26 nm) along the crystal *c*-axis and their channel entrances end only at the base of the crystal.[3] Due to its versatile properties, zeolite L can be functionalized in various ways and has gained increasing interest as a base for innovative materials.[4] For example, incorporation of organic molecules and metal complexes such as dyes or drugs into the channels leads to stable pigments or agent carriers.[5] As one of the first groups recognizing the high potential of zeolite L, Calzaferri *et al.* developed methods for specific zeolite surface functionalization.[5a,6] Furthermore, it was shown by De Cola *et al.* as well as by our group that modified zeolite L crystals can self-assemble by utilizing either complexation[7] or reversible covalent bond formation between complementary functionalized crystals.[4d,e] De Cola *et al.* also documented that amino-functionalized and therefore positively charged zeolite L crystals can assemble with living cells.[6f,8] Recently, we have shown that this electrostatic-type binding can be exploited for the controlled fabrication of such bio-hybrid systems with holographic optical tweezers (HOT),[4b,9] by which multiple optical traps can be generated for the simultaneous manipulation of several zeolite L crystals or motile bacteria in a contactless and thus, minimally invasive way.[10]

Surprisingly, only a few papers dealing with zeolite L/polymer hybrid materials have appeared to date. Notably, this type of organic/inorganic hybrid system should combine the properties of the versatile inorganic zeolite L core material and also those of the functional soft polymers. After demonstrating that non-functionalized zeolite L crystals can be incorporated into polymer fibers *via* electrospinning,[6e] Botta *et al.* also showed that negatively charged zeolites can aggregate into well-defined fiber-like structures after complexation with cationic polymers.[6i] Calzaferri *et al.* reported covalent attachment of polymers to the zeolite L surface by copolymerizing methyl methacrylate (MMA) and methacrylate-functionalized crystals as macro cross-linkers.[6g] Taking advantage of the host–guest behavior then leads to various transparent organic/inorganic hybrid materials showing interesting properties.[11]

To the best of our knowledge, polymer coated zeolite L hybrid materials prepared in a grafting-from process by surface initiated radical polymerization are unknown. It is obvious that the polymer shell in these core–shell systems will readily allow for tuning surface properties.[12]

Herein, we present the synthesis of zeolite L based polymer brush particles. Alkoxyamine- and α-bromoisobutyrate-functionalized zeolite L crystals are utilized as macroinitiators for surface initiated nitroxide mediated polymerization (siNMP)[13] and surface initiated atom transfer radical polymerization (siATRP).[12] To document the success of polymerization and as evidence for controllable polymer chain length and therefore surface concentration of functionalities, a fluorescent model polymer is used. We demonstrated recently, that polymers bearing 2-hydroxy-2-methyl-1-phenylpropan-1-one as backbone substituents can be cleaved in a Norrish-Type-I photoreaction to generate acyl radicals that can trap persistent radicals such

[a]*Westfälische Wilhelms-Universität Münster, Organic Chemistry Institute, Corrensstrasse 40, 48149 Münster, Germany. E-mail: studer@uni-muenster.de*
[b]*Westfälische Wilhelms-Universität Münster, Institute of Applied Physics, Corrensstrasse 2-4, 48149 Münster, Germany. E-mail: denz@uni-muenster.de*
†Electronic supplementary information (ESI) available. See DOI: 10.1039/c5py00425j

as nitroxides in excellent yields.[14] This led to a novel efficient approach for postmodification of polymers and polymer brushes in a modular manner. Along these lines, we will discuss herein the synthesis of hybrid particles containing acyloin moieties in their polymer layer that can be photochemically postmodified. The potential of this methodology is documented by the successful preparation of a small representative library of differently functionalized zeolite L crystals.

Importantly, as compared to zeolite L crystals that are functionalized with monolayers, brush-type zeolites as reported herein possess a much higher surface concentration of functionalities, a higher dispersibility in various solvents,[6d] and also softer surfaces. Potential applications of this novel type of zeolite L material fall within the scope of medicine and biology, optics and photonics or microelectronics for example. Utilizing the host–guest behavior of zeolite L in combination with highly functionalized polymer shells is interesting for drug delivery and release. Also incorporation of photo-active guests into the strictly parallel channel structure results in Förster resonance energy transfer (FRET) within the crystal[6a,h] and tuning the surface properties by polymer chemistry can facilitate its utilization in OLEDs or organic solar cells for instance. In general these core–shell particles can be readily incorporated into different polymer materials by established macromolecular chemistry and due to the special advantages of zeolite L, micro- and macroscopic properties of these materials can be adjusted.

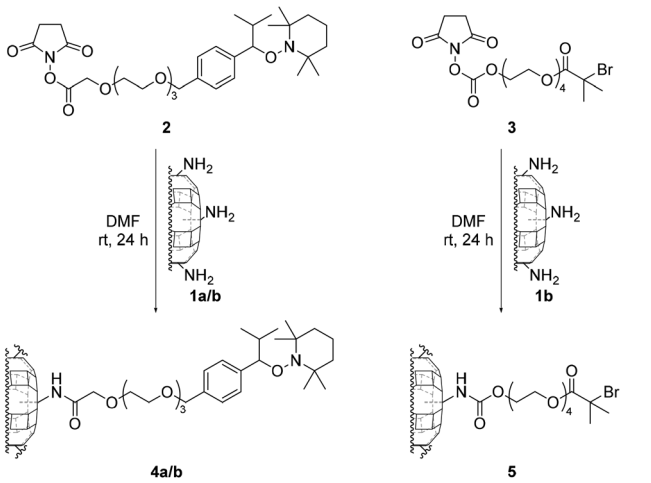

Scheme 1 Synthesis of macroinitiators **4a/b** and **5**.

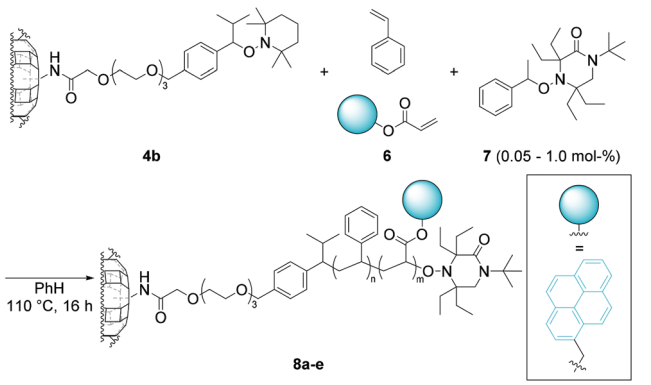

Scheme 2 Synthesis of fluorescent zeolite L based polymer brushes **8a–e** *via* siNMP.

Results and discussion

Preparation of zeolite L based polymer brushes

Zeolite L crystals of about 1 μm diameter and 1 μm or 4 μm length were all-over functionalized with (3-aminopropyl) triethoxysilane (APTES) by dispersing the crystals in toluene and heating the mixture in the presence of an excess APTES to obtain amino-functionalized particles **1a** (1 μm) and **1b** (4 μm). Successful surface modification was supported by zeta potential (ζ) measurements in ammonium formate buffer (AFB, 20 mM, pH = 7.4, 25 °C), revealing a positive potential of ζ_{1a} = +34.5 mV and ζ_{1b} = +41.9 mV. Subsequent amidation of the surface-bound amines in **1a** and **1b** with active esters of NMP- and ATRP-initiators **2** and **3** resulted in macroinitiators **4a/b** and **5**, respectively (Scheme 1).

A fluorescent model polymer bearing pyrene moieties was used to study and document the success of the surface initiated polymerization *via* fluorescence microscopy. To this end, pyren-1-ylmethyl acrylate (**6**) was prepared from pyrene-1-carbaldehyde by LAH-reduction and subsequent acylation. Following standard protocols,[13] siNMP macroinitiator **4b** was reacted with styrene/pyrene monomer **6** (12 : 1) and alkoxyamine **7**[15] (0.05–1.0 mol%) at 110 °C for 16 h to give hybrid materials of type **8** (Scheme 2). The addition of alkoxyamine **7** as a sacrificial initiator is essential since the polymerization control would be impaired due to the low overall concentration of surface-bound alkoxyamines.[16] In addition, polymers formed upon initiation by the unbound alkoxyamine **7** can be used to estimate molecular weight (M_n) and polydispersity index (PDI) of the surface bound polymers by using gel permeation chromatography (GPC), assuming that unbound and surface-bound polymer chains react comparably and therefore grow uniformly.[13] Due to the narrow pore size (0.76–1.26 nm) we assume that there is no efficient polymer growth inside the crystals but only at the outer surface. For analysis the reaction mixture was centrifuged and washed with THF three times to separate polymer brushes **8a–e** and unbound polymers.

As expected increasing the concentration of the sacrificial initiator **7** leads to lower molecular weights of the unbound polymers (Table 1) and a decreased fluorescence activity of the core–shell particles **8a–e** (Fig. 1), which indicates control over the polymer chain length as a function of the concentration of **7**. The incorporation ratio of styrene/pyrene acrylate **6** into the unbound polymer is around 8 : 1 for each concentration of **7** according to ^{1}H NMR analysis of the corresponding signals. This proves that the initiator concentration and therefore the

Table 1 Influence of the initiator concentration on the polymer brush synthesis *via* siNMP

Entry	Zeolite	7/ mol%	Conv./ %	$M_{n,theo.}$/ kg mol^{-1}	$M_{n,exp.}$/ kg mol^{-1}	PDI
1	**8a**	0.05	50	120	67	1.23
2	**8b**	0.10	56	66	38	1.22
3	**8c**	0.25	61	29	17	1.12
4	**8d**	0.50	60	14	11	1.13
5	**8e**	1.00	25	3.0	2.9	1.15

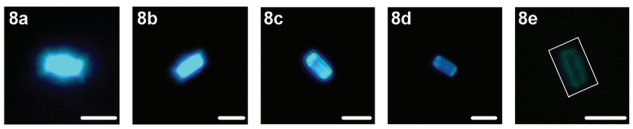

Fig. 1 Fluorescence images of core–shell particles **8a–e** synthesized by siNMP with decreasing fluorescence activity. Scale bars are 4 μm.

chain length is not effecting the incorporation ratio of the two different monomer types.

Molecular weights M_n ranging from 67 kg mol^{-1} to 2.9 kg mol^{-1} with PDIs from 1.12 to 1.23 were measured by GPC. Notably, we found that the oligoethylene glycol linker is essential for success of the surface initiated polymerization. For particles of type **4a/b** lacking the PEG-linker, siNMP failed. We assume that shorter or no linkers result in macroinitiator deactivation by dimerization of the initiating transient radicals due to surface radical confinement.

In analogy, α-bromoisobutyrate-functionalized zeolite L crystals **5** were converted with MMA/pyrene acrylate **6** (12 : 1) using ethyl α-bromoisobutyrate (**9**, EBiB, 0.1 mol%) as an external initiator[16] and $CuBr_2$/tris[2-(dimethylamino)ethyl]amine (Me_6TREN) in combination with ascorbic acid as a catalyst system[17] at 50 °C for 6 h to hybrid particles of type **10** (Scheme 3). Particles **10** and unbound polymers were separated in three centrifugation–washing cycles in THF and GPC analysis of the unbound polymer revealed an estimated molecular weight M_n for the brush polymers of 59 kg mol^{-1} with a PDI of 1.31. The incorporation ratio of MMA/pyrene acrylate **6** into the unbound polymer is around 18 : 1 according to ^{1}H NMR analysis of the corresponding signals. As expected for brush materials containing **6**, strong fluorescence was observed for the organic/inorganic hybrid **10**.

Photo-postmodification of polyacyloin brush particles

Previous studies in our group revealed that polymeric acyl radicals generated *via* a Norrish-Type-I reaction are quantitatively trapped by persistent nitroxide radicals. We therefore decided to run siNMP with a styrene derivative bearing an acyloin entity resulting in a polyacyloin brush material that should be readily activated by UV light (λ = 365 nm) and postmodified *via* spin trapping using various functionalized nitroxides.[14] This approach will allow us to readily prepare a library of functionalized zeolite L/polymer hybrid particles in a modular approach starting with a single type of mother zeolite particle.

The photo-cleavable monomer 2-hydroxy-2-methyl-1-(4-vinylphenyl)propan-1-one (**11**) was prepared according to a literature procedure.[14b] siNMP-active zeolite **4a** was reacted with styrene/styrene derivative **11** (4 : 1) and alkoxyamine **7** (0.1 mol%) at 110 °C for 16 h to provide photo-postmodifiable zeolites **12** with an estimated M_n of 74 kg mol^{-1} and a PDI of 1.21, as determined by GPC analysis of the unbound polymer (Scheme 4).

To show the diversity of our modular zeolite L modification approach a variety of functionalized nitroxides **13–19** was used for the photo trapping reaction (Fig. 2). 2,2,6,6-Tetramethylpiperidine-1-oxyl (**13**, TEMPO) is commercially available. Nitroxides **14–19** were synthesized according to the cited literature.[4c,18]

Photo-postmodification was conducted with zeolites **12** (15 mg) and an excess of the respective nitroxides **13–19** (2.0 mg) in DMF (0.3 mL) using a LED (λ = 365 nm, 3 mW) at room temperature for 1 h (Scheme 5).[19]

Excess starting materials and byproducts were removed in several centrifugation–washing cycles (see the Experimental section for details). Success of the postmodification was

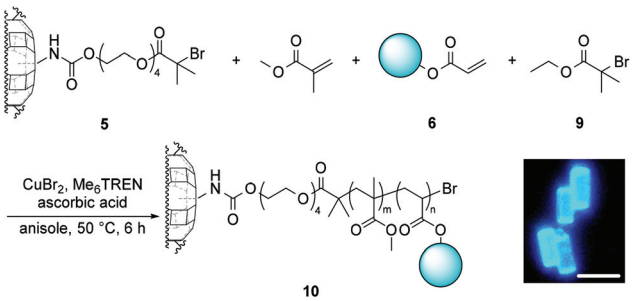

Scheme 3 Synthesis of fluorescent zeolite L based polymer brushes **10** *via* siATRP. Scale bar is 4 μm.

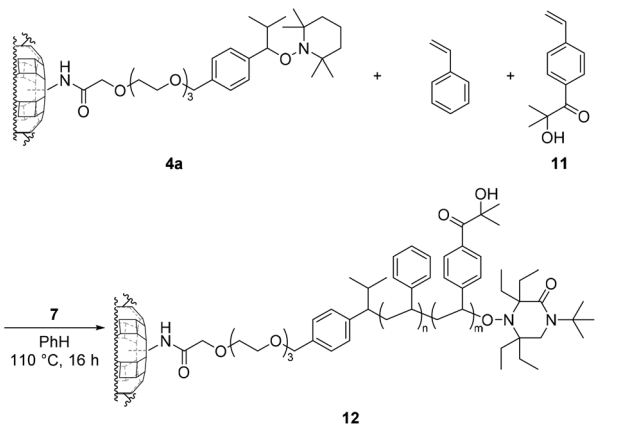

Scheme 4 Synthesis of photo-postmodifiable polymer brushes **12** *via* siNMP.

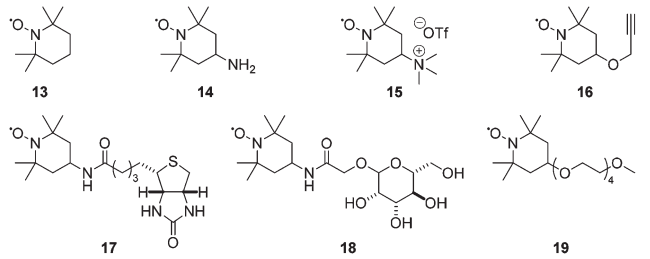

Fig. 2 Functionalized nitroxides **13–19** used for the photo-postmodification.

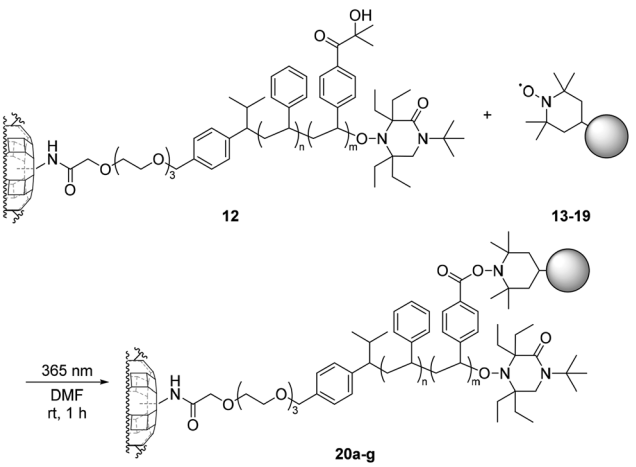

Scheme 5 Photo-postmodification of **12** with nitroxides **13–19**.

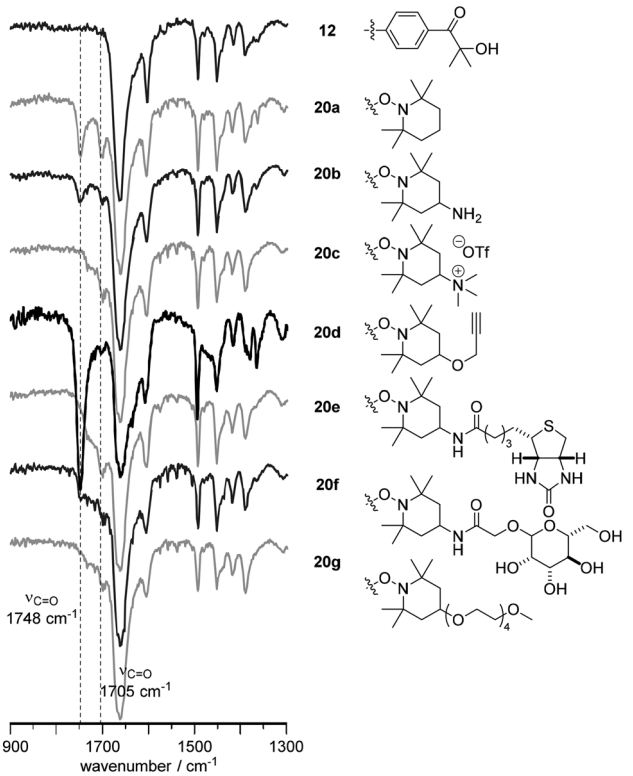

Fig. 3 IR -spectra of **12** and photo-postmodified zeolites **20a–g**.

proved by IR-analysis and zeta potential measurements before and after photochemical modification.

Based on the fact that conversion of the photo-active moiety in polymers to TEMPO esters in solution occurs quantitatively based on NMR analysis,[14b] we assume that the surface bound photoactive moieties are also activated and trapped in high yield. IR spectra of the resulting particles **20a–g** were recorded and new peaks at 1705 and 1748 cm^{-1} were assigned to the C═O stretching mode of the **TEMPO** ester moiety which was not present in the starting particles **12** indicating successful ester formation (Fig. 3).[14a,b] The amide carbonyl stretching band expected in materials **20e/f** is hidden below the large band of the zeolite at around 1663 cm^{-1}. Unfortunately, due to peak overlap we were not able to quantify the chemical postmodification. However, based on our previous reports we expect the modification to occur in high yields.[14a,b]

Zeta potentials ζ of zeolite L crystals **20a–g** measured in AFB (20 mM, pH = 7.4, 25 °C) are summarized in Table 2.

Polyacyloin brush particles **12** show a negative potential of ζ = −30.4 mV (entry 1). Functionalization with neutral to partially negatively charged nitroxides **13** and **16–19** leads to particles **20a** and **20d–g** which feature only a slightly changed potential (entries 2, 5–8). Attachment of 4-amino-TEMPO (**14**) provides particles **20b** that are protonated within the buffered medium and therefore positively charged (ζ = +15.9 mV, entry 3). Zeolites **20c** show a strong positive charge of ζ = +38.4 mV which supports successful conjugation of **15** to the zeolite L crystal (entry 4).

To prove necessity of the acyloin moiety together with irradiation and refute non-specific binding, the following control experiments were conducted. Polystyrene brush particles were synthesized in the absence of monomer **11** and reacted with 4-amino-TEMPO (**14**) following the general procedures. Polyacyloin brush particles **12** were incubated with nitroxide **14** in the absence of light. Both control experiments show no changes regarding IR absorption, ζ-potential or fluorescence activity after subsequent labeling (see the ESI† for details). Thus, specificity of the reported approach is proven.

In particular, positively charged zeolite L crystals **20c** are especially interesting for the realization of bacteria–zeolite L hybrid systems, where the positively charged zeolite L surface binds electrostatically to living bacteria, which feature a negatively charged cell envelope.[20] Recently, we have demonstrated that such bio-hybrid assemblies can be finely fabricated using HOT.[4b] By means of this optical approach, we show the capability of zeolites **20c** to get attached to living bacteria using as a model of bacteria a wild type strain of self-propelling rod-shaped *Bacillus subtilis* in chemotaxis buffer and therefore demonstrate one possible application of this novel type of zeolite L material (Fig. 4).

Finally, photochemically postmodified non-fluorescent zeolites **20b,d–f** were reacted with various fluorophores to obtain

Table 2 Zeta potentials of photo-functionalized zeolites **20a–g** in AFB (20 mM, pH = 7.4, 25 °C)

Entry	1	2	3	4	5	6	7	8
Nitroxide	—	**13**	**14**	**15**	**16**	**17**	**18**	**19**
Zeolite	**12**	**20a**	**20b**	**20c**	**20d**	**20e**	**20f**	**20g**
ζ/mV	−30.4	−43.9	15.9	38.4	−27.6	−40.2	−38.8	−25.2

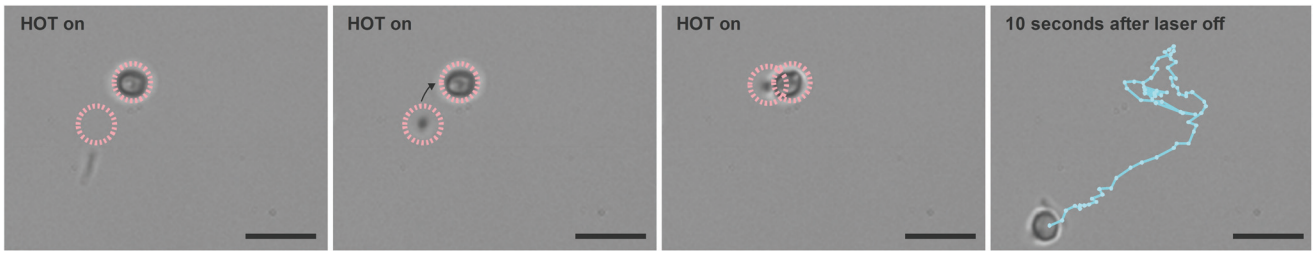

Fig. 4 Optical microscopy images that show the optical assembly of **20c** and self-propelling *B. subtilis* with HOT (red circles). The dashed red circles indicate the position of the dynamic optical traps. After turning off the HOT laser, the bacterial cell carries the particle along the blue trajectory. Scale bars are 2 μm.

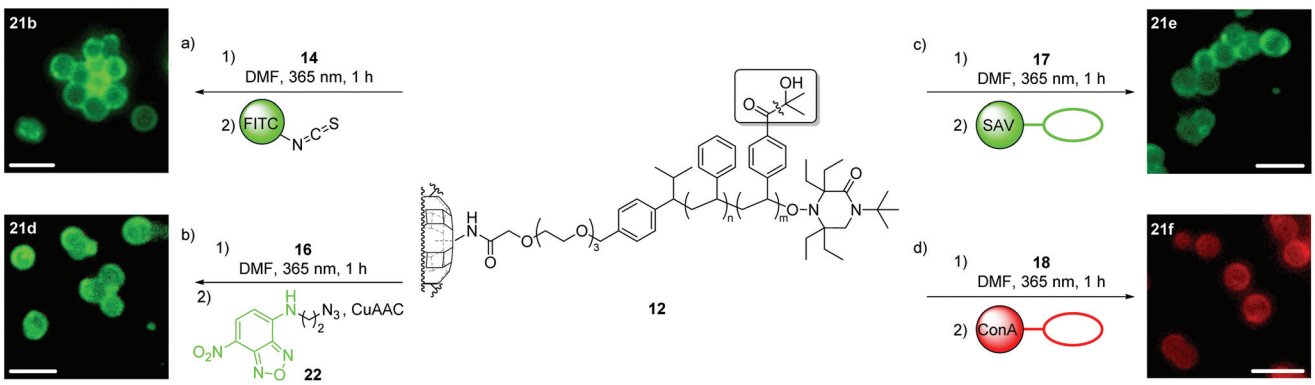

Scheme 6 Photo-postmodification and fluorescence labeling of zeolite L based polymer brushes **12**: (a) FITC conjugation; (b) CuAAC-click reaction; (c) immobilization of labeled SAV; (d) attachment of ConA. Scale bars are 2 μm.

zeolites **21b,d–f** which were analyzed *via* fluorescence microscopy after several centrifugation–washing cycles to support successful modification (Scheme 6). Along these lines, amino-functionalized zeolites **20b** were reacted with fluorescein isothiocyanate (FITC) to afford fluorescent particles **21b** (Scheme 6a). The alkyne-functionalized crystals **20d** were successfully conjugated *via* copper(I)-catalyzed azide–alkyne cycloaddition (CuAAC) with *N*-(2-azidoethyl)-7-nitrobenzo[*c*][1,2,5]oxadiazol-4-amine (**22**) to give strongly fluorescent zeolite crystals **21d** (Scheme 6b). Biotin-conjugated crystals **20e** upon immersion with fluorophore-labeled streptavidin (SAV) resulted in intense green fluorescent protein decorated particles **21e** (Scheme 6c). Similarly, glycoconjugated crystals **20f** were recognized by rhodamine-labeled concanavalin A (ConA) to afford red fluorescent zeolite L crystals **21f** containing ConA at the surface (Scheme 6d). Control experiments were conducted by immediate treatment of **12** with fluorophores under respective conditions without preceding photo-modification to disprove non-specific adsorption (see the ESI† for details). Reaction of **12** with FITC or **22** leads to particles showing barely any fluorescence proving that there is no non-specific binding of these fluorophores. Immobilization of labeled SAV or ConA onto **12** results in comparatively weak fluorescent particles. Remaining residual adsorption of the proteins might occur from non-specific adsorption due to interactions with the polystyrene part of the polymer shell, but clearly protein decoration is highly increased by preceding conjugation of the respective biomolecules.

Conclusion

In summary, we have successfully prepared novel types of zeolite L/polymer hybrid materials by a straightforward modular approach comprising surface initiated radical polymerization and subsequent photochemical postmodifica-

tion. Zeolite L based photo-active polymer brushes were generated in a grafting-from process using zeolite L crystals as macroinitiators for siNMP and siATRP. Copolymerization with a fluorescent monomer resulted in fluorescent brushes where the molecular weight of the surface attached polymers and hence the fluorescence intensity can be adjusted. Surface initiated copolymerization of styrene with a photo-cleavable monomer results in photoactive brushes that can be readily photochemically modified by UV irradiation in the presence of functionalized nitroxides to afford the corresponding modified polymer brush particles. With the robust photochemistry, various functionalities can be introduced at the surface without the need of any protecting group strategies. For example, introduction of quaternized ammonium groups resulted in positively charged particles which were then used for the optical tweezer-assisted fabrication of bio-hybrid microrobots. Also biotin or non-protected glucose was readily conjugated to the surface bound polymers. Moreover, alkynyl groups can be introduced which can be further chemically modified *via* established click chemistry. Importantly, our method features robustness in terms of late stage functionalization and due to the polymeric nature of the modifiable units, a high density of functionalities at the surface can be achieved in these novel organic/inorganic hybrid systems.

Experimental

General information

Zeolite L crystals were either purchased from Süd-Chemie (1.0–1.5 × 1.0 μm) or synthesized following reported procedures[21] (4.0 × 1.0 μm). Reagents were purchased from ABCR, Aldrich, Acros Organics, Alfa Aesar, Merck or TCI and used as received. Rhodamine-labeled ConA (5.0 mg mL^{-1} in HEPES buffer) was purchased from VECTOR Laboratories and Oyster®-488-tagged SAV (1.0 mg mL^{-1} in PBS buffer) from Luminartis. Styrene and MMA were destabilized by distillation over CaH_2. Reactions were carried out in heat-gun-dried flasks under an Ar atmosphere and by using standard Schlenk techniques. GPC was carried out in degassed THF as the eluent with a flow rate of 1.0 mL min^{-1} at rt on a system consisting of a Knauer HPLC Pump 64, a set of two PLgel 5 μm MIXED-C columns (300 × 7.5 mm, Polymer Laboratories) and a Shodex RI differential refractometer detector. Calibration was performed with a Varian polystyrene (PS) calibration kit, PL2010-0100, S-M-10, Lot 103. Signals of the PS standards ranged from M_n = 1530 to 1 319 000 g mol^{-1}. Data analysis was performed with Polymer Standards Service WinGPC Compact V.7.20 software. Fluorescence images were recorded on an epifluorescence microscope Olympus reflected fluorescence system CKX41 with a Lumen Dynamics X-Cite Series 120Q excitation source, excitation/emission filters and an Olympus U-LS30-3 camera. IR spectra were recorded on a Digilab FTS 4000 equipped with a MKII Golden Gate single reflection ATR system. ζ-Potentials were measured on a Malvern DTS Zetasizer Nano ZS using the Smoluchowski equation. HOT experiments were performed on an inverted fluorescence microscope Nikon Eclipse Ti with a high numerical aperture microscope objective (Nikon Apo TIRF, 100×/1.49 Oil-immersion) and a Nd:YVO_4 laser (λ = 1064 nm, power at sample plane 400 mW approx.) as the light source for optical trapping. The implemented HOT system is described in detail in the literature.[4b] ^1H and ^{13}C NMR spectra were recorded on a Bruker DPX 300 (300 MHz; at 298 K). Chemical shifts δ are noted in ppm and relatively to ^1H or ^{13}C signals of tetramethylsilane (0.0 ppm). Spectra are referenced to the solvent residual peak. High resolution mass spectra (HRMS) were recorded on a Bruker Daltonics MicroTof after electrospray ionization (ESI). Detected m/z signals are given in u. Melting points (MP) were determined on a Stuart SMP10 and are uncorrected.

Active esters **2**[4e] and **3**,[22] alkoxyamine **7**,[15] styrene derivative **11**,[14b] nitroxides **14**,[18a] **15**,[18b,c] **16**,[18d] **17**,[4c] **18**[4c] and **19**[18a] were prepared according to literature procedures.

General procedure for amino-functionalization of zeolite L

Unmodified zeolite L crystals (**a**: 1.0–1.5 × 1.0 μm; **b**: 4.0 × 1.0 μm) were dispersed in dry toluene (c = 100 mg mL^{-1}) and an excess of APTES (c = 100 μl mL^{-1}) was added. The suspension was sonicated for 3 min and stirred at 85 °C for 4 h. The mixture was centrifuged, the supernatant decanted and the residue washed three times with Et_2O in subsequent centrifugation–washing cycles. Functionalized crystals **1a/b** were dried under reduced pressure.

ζ-Potential in ammonium formate buffer (AFB, 20 mM, pH = 7.4, 25 °C): $\zeta_{\mathbf{1a}}$ = +34.5 mV, $\zeta_{\mathbf{1b}}$ = +41.9 mV.

General procedure for functionalization of zeolite L with active esters 2 and 3

Amino-functionalized zeolite L crystals **1a/b** were dispersed in DMF (c = 50 mg mL^{-1}) and sonicated for 5 min. The respective active ester solution of **2** or **3** in DMF (50 mM) was added in excess and the suspension was stirred at rt for 24 h. The mixture was centrifuged, the supernatant decanted and the residue washed three times with Et_2O in subsequent centrifugation–washing cycles. Functionalized crystals **4a/b** or **5** were dried under reduced pressure.

Synthesis of pyren-1-ylmethyl acrylate (6)

Pyren-1-ylmethanol. A solution of pyrene-1-carbaldehyde (2.30 g, 10.0 mmol, 1.0 eq.) in THF (10 mL) was cooled to 0 °C and $LiAlH_4$ (417 mg, 11.0 mmol, 1.1 eq.) was added portionwise. The mixture was stirred at 0 °C for 10 min and at rt for 1 h. The reaction was quenched by addition of H_2O (0.5 mL), NaOH (aq., 4.0 M, 0.5 mL) and H_2O (1.0 mL). The suspension was filtered, the residue washed with THF (30 mL) and the filtrate evaporated *in vacuo*. Pyren-1-ylmethanol was obtained as a yellow solid (2.33 g, 10.0 mmol, quant.) and used without further purification.

Pyren-1-ylmethyl acrylate (6). A solution of pyren-1-ylmethanol (2.33 g, 10.0 mmol, 1.00 eq.) and acryloyl chloride (950 mg, 850 μL, 10.5 mmol, 1.05 eq.) in CH_2Cl_2 (80 mL) was cooled to 0 °C and Et_3N (1.21 g, 1.66 mL, 12.0 mmol, 1.20 eq.) was added. The mixture was stirred at rt for 18 h. H_2O (80 mL)

was added and the aqueous phase was extracted with CH_2Cl_2 (3 × 50 mL). The combined organic layers were dried over $MgSO_4$ and the solvent was removed *in vacuo*. Purification by flash chromatography (pentane/Et_2O = 14 : 1 → 9 : 1) provided acrylate **6** as a pale yellow solid (2.47 g, 8.63 mmol, 86%).

^{1}H NMR (300 MHz, $CDCl_3$, 298 K): δ = 8.32–7.99 (m, 9H, $CH_{arom.}$); 6.48 (dd, ^3J = 17.3 Hz, ^2J = 1.5 Hz, 1H, C=C*H*H); 6.20 (dd, ^3J = 17.3 Hz, ^3J = 10.4 Hz, 1H, CH); 5.93 (s, 2H, CH_2); 5.85 (dd, ^3J = 10.4 Hz, ^2J = 1.5 Hz, 1H, C=CH*H*). ^{13}C NMR (75 MHz, $CDCl_3$, 298 K): δ = 166.2 (C_q), 131.9 (C_q), 131.3 (CH_2), 131.3 (C_q), 130.8 (C_q), 129.7 (C_q), 128.9 (C_q), 128.5 (CH), 128.3 (CH), 127.9 (CH), 127.8 (CH), 127.4 (CH), 126.2 (CH), 125.6 (CH), 125.5 (CH), 125.0 (C_q), 124.8 (C_q), 124.7 (CH), 123.0 (CH), 64.91 (CH_2). HRMS (ESI) calculated for $C_{20}H_{14}O_2Na^+$ ([M + Na]$^+$): 309.0886. Found: 309.0879. Analytical data are in accordance with the literature data.[23]

General procedure for preparation of polymer brush particles *via* siNMP

Alkoxyamine-modified zeolite L crystals **4a/b** (c = 10 mg mmol$_{monomer\ mixture}^{-1}$), functional monomer **6** or **11** (n = 0.08–0.2 eq.), styrene (1.0–n eq.) and alkoxyamine **7** (0.05–1.0 mol%) were added to benzene (c = 50 μL mmol$_{monomer\ mixture}^{-1}$). The suspension was degassed in three freeze–thaw cycles, sonicated for 3 min and stirred at 110 °C for 16 h. Polymer brush particles and unbound polymers were separated in three centrifugation–washing cycles with THF (3 × 10 mL) and solvents were evaporated *in vacuo*. The unbound polymer was dissolved in a minimum amount of CH_2Cl_2, precipitated from methanol and dried *in vacuo*.

GPC data are summarized in Table 1.

General procedure for preparation of polymer brush particles *via* siATRP

α-Bromoisobutyrate-functionalized zeolite L crystals **5** (2.0 mg), pyrene acrylate **6** (23 mg, 80 μmol, 0.08 eq.) and MMA (98 μL, 0.92 mmol, 0.92 eq.) were added to EBiB (stock solution in anisole, 20 mM, 50 μL, 1.0 μmol, 0.1 mol%) and $CuBr_2$/Me_6TREN (stock solution in anisole, c_{CuBr_2} = 2.0 mM, c_{Me_6TREN} = 20 mM, 200 μL, n_{CuBr_2} = 0.4 μmol, n_{Me_6TREN} = 4.0 μmol, 0.04 mol%/0.4 mol%). The suspension was degassed in three freeze–thaw cycles and sonicated for 3 min. Ascorbic acid (0.2 mg, 1 μmol, 0.1 mol%) was added and the suspension was stirred at 50 °C for 6 h. Polymer brush particles **10** and unbound polymers were separated in three centrifugation–washing cycles with THF (3 × 10 mL) and solvents were evaporated *in vacuo*. The unbound polymer was dissolved in a minimum amount of THF, filtered through a short plug of silica, precipitated from methanol and dried *in vacuo*.

GPC: M_n = 59 kg mol^{-1}; PDI = 1.31.

General procedure for photo-postmodification of zeolite L based polyacyloin brushes with nitroxides 13–19

Polyacyloin brush particles **12** (15 mg) were dispersed in DMF (0.3 mL) and the respective nitroxides **13–19** (2.0 mg, excess) were added to the suspension. The mixture was sonicated for 3 min and stirred under LED irradiation (λ = 365 nm, 3 mW) at rt for 1 h. Polymer brush particles **20a–g** were washed in four centrifugation–washing cycles with DMF (2.0 mL), MeOH (2 × 2.0 mL) and DCM (2.0 mL) and dried *in vacuo*.

ζ-Potentials in AFB (20 mM, pH = 7.4, 25 °C) are summarized in Table 2.

General procedure for preparation of HOT experimental samples

Zeolite L crystals **20c** (c = 0.1 mg mL^{-1}) were dispersed in a chemotaxis buffer (10 mM K_2HPO_4/KH_2PO_4 buffer (pH = 7.0), 0.14 mM $CaCl_2$, 0.30 mM $(NH_4)_2SO_4$, 0.10 mM EDTA (pH = 5.0), 5.0 mM sodium lactate, 0.05% glycerol) by sonication for 5 min. *B. subtilis* were washed with chemotaxis buffer in three centrifugation–washing cycles, dispersed in chemotaxis buffer and added to the zeolite suspension. One droplet of the mixture was applied on a microscope slide.

General procedure for FITC conjugation

Amino-functionalized zeolite L **20b** (2.0 mg) was dispersed in DMF (2.0 mL) and FITC (1.0 mg, 3.6 μmol, excess) and Et_3N (10 μL, 72 μmol, excess) were added. The suspension was sonicated for 3 min and stirred at rt for 2 h. Polymer brush particles **21b** were washed in five centrifugation–washing cycles with DMF (2.0 mL), MeOH (2 × 2.0 mL) and DCM (2 × 2.0 mL) and dried *in vacuo*.

Synthesis of *N*-(2-azidoethyl)-7-nitrobenzo[*c*][1,2,5]oxadiazol-4-amine (22)

N-(2-Bromoethyl)-7-nitrobenzo[c][1,2,5]oxadiazol-4-amine. 4-Chloro-7-nitrobenzo[*c*][1,2,5]oxadiazole (100 mg, 500 μmol, 1.0 eq.) was dissolved in EtOAc (3.0 mL). 2-Bromoethylammonium chloride (102 mg, 500 μmol, 1.0 eq.) and $NaHCO_3$ (126 mg, 1.50 mmol, 3.0 eq.) were added and the suspension was stirred at 40 °C for 23 h. The mixture was filtered and the residue was washed with CH_2Cl_2 (20 mL). HCl (aq. 1 M, 15 mL) was added to the filtrate and the aqueous phase was extracted with CH_2Cl_2 (3 × 20 mL). The combined organic layers were dried over $MgSO_4$ and solvents were removed *in vacuo*. Purification by flash chromatography (pentane/Et_2O = 1 : 1) provided *N*-(2-bromoethyl)-7-nitrobenzo[*c*][1,2,5]oxadiazol-4-amine as a red solid (105 mg, 366 μmol, 73%).

MP: 129 °C. ^{1}H NMR (300 MHz, $CDCl_3$, 298 K): δ = 8.50 (d, ^3J = 8.5 Hz, 1H, $CH_{arom.}$); 6.39 (s, 1H, NH); 6.26 (d, ^3J = 8.5 Hz, 1H, $CH_{arom.}$); 4.04–3.88 (m, 2H, CH_2N); 3.70 (t, ^3J = 6.0 Hz, 2H, CH_2Br). IR (film): 3336w, 3094w, 2463w, 1618m, 1562s, 1527m, 1495s, 1460w, 1432m, 1385w, 1351w, 1330m, 1247s, 1174m, 1141m, 1061w, 1003m, 899m, 825m, 779m, 738m, 675w cm^{-1}. HRMS (ESI) calculated for $C_8H_7BrN_4O_3Na^+$ ([M + Na]$^+$): 308.9594. Found: 308.9621.

N-(2-Azidoethyl)-7-nitrobenzo[c][1,2,5]oxadiazol-4-amine (22). *N*-(2-Bromoethyl)-7-nitrobenzo[*c*][1,2,5]oxadiazol-4-amine (40 mg, 0.14 μmol, 1.0 eq.) and NaN_3 (27 mg, 0.42 μmol, 3.0 eq.) were dissolved in DMF (2.0 mL). The mixture was stirred at 80 °C for 4 h and at rt for 15h. H_2O (10 mL) was added, the aqueous phase was extracted with Et_2O (5 × 20 mL), the combined

organic layers were dried over $MgSO_4$ and the solvents were removed *in vacuo*. Purification by flash chromatography (pentane/Et_2O = 1 : 2 → 1 : 3) provided azide **22** as an orange solid (33 mg, 0.13 mmol, 95%).

MP: 136 °C. ^{1}H NMR (300 MHz, DMSO-d_6, 298 K): δ = 9.49 (bs, 1H, NH); 8.52 (d, ^3J = 8.8 Hz, 1H, $CH_{arom.}$); 6.51 (d, ^3J = 8.9 Hz, 1H, $CH_{arom.}$); 3.69 (bs, 4H, 2 × CH_2). IR (film): 3226m, 3152w, 3098w, 3070w, 3002w, 2957w, 2119s, 2056w, 1616m, 1585s, 1529m, 1499s, 1448m, 1413m, 1368w, 1348m, 1293s, 1280s, 1250s, 1213s, 1192m, 1127s, 1091m, 1064m, 1035m, 998m, 985m, 927w, 900m, 838m, 812m, 778m, 740m, 679w, 640m cm^{-1}. HRMS (ESI) calculated for $C_8H_7N_7O_3Na^+$ ($[M + Na]^+$): 272.0503. Found: 272.0503.

General procedure for CuAAC

Alkyne-functionalized zeolite L **20d** (2.0 mg) was dispersed in THF (0.2 mL) and H_2O (0.1 mL). Azide **22** (1.0 mg, 4.0 μmol, excess), sodium ascorbate (1.0 mg, 3.6 μmol, excess) and $CuSO_4$ (~0.1 mg) were added. After degasification with an Ar stream the suspension was sonicated for 3 min and stirred at rt for 4 h. Polymer brush particles **21d** were washed in five centrifugation–washing cycles with MeOH (5 × 2.0 mL) and dried *in vacuo*.

General procedure for immobilization of fluorophore labeled proteins

Modified zeolite L crystals **20e** or **20f** (1.0 mg) were dispersed in H_2O (0.2 mL) by sonication for 3 min and an excess of the respective protein buffer solution (2.0 μL) was added. The suspension was stirred at rt for 4 h. Polymer brush particles **21e** or **21f** were washed in five centrifugation–washing cycles with H_2O (5 × 2.0 mL) and dried *in vacuo*.

General procedure for preparation of fluorescence samples

For fluorescence analysis particles were dispersed in toluene (c = 2 mg mL^{-1}) by sonication for 1 min. One droplet of this suspension was wept onto a microscope cover slip using a pipette and the solvent was evaporated at rt.

Acknowledgements

This work was supported by the Deutsche Forschungsgemeinschaft within the framework of the Sino-German-TRR 61. The Fonds der Chemischen Industrie is acknowledged for a fellowship (T.B.). The authors would like to thank Berenike Maier, University of Cologne, for kindly providing *B. subtilis* samples.

Notes and references

1 Database of zeolite structures, http://www.iza-structure.org/databases, 2015.

2 (*a*) R. Le Van Mao, N. T. Vu, S. Xiao and A. Ramsaran, *J. Mater. Chem.*, 1994, **4**, 1143–1147; (*b*) T. P. Vispute, H. Zhang, A. Sanna, R. Xiao and G. W. Huber, *Science*, 2010, **330**, 1222–1227; (*c*) G. Bellussi, A. Carati, C. Rizzo and R. Millini, *Catal. Sci. Technol.*, 2013, **3**, 833–857; (*d*) K. Na, M. Choi and R. Ryoo, *Microporous Mesoporous Mater.*, 2013, **166**, 3–19.

3 R. M. Barrer and H. Villiger, *Z. Kristallogr.*, 1969, **128**, 352–370.

4 (*a*) Y. Yan, X. Guo, Y. Zhang and Y. Tang, *Catal. Sci. Technol.*, 2015, **5**, 772–785; (*b*) Á. Barroso, S. Landwerth, M. Woerdemann, C. Alpmann, T. Buscher, M. Becker, A. Studer and C. Denz, *Biomed. Microdevices*, 2015, **17**, 1–8; (*c*) M. Becker, L. De Cola and A. Studer, *Chem. Commun.*, 2011, **47**, 3392–3394; (*d*) M. Becker, L. De Cola and A. Studer, *J. Mater. Chem. C*, 2013, **1**, 3287–3290; (*e*) B. Schulte, M. Tsotsalas, M. Becker, A. Studer and L. De Cola, *Angew. Chem., Int. Ed.*, 2010, **49**, 6881–6884; (*f*) M. Veiga-Gutiérrez, M. Woerdemann, E. Prasetyanto, C. Denz and L. De Cola, *Adv. Mater.*, 2012, **24**, 5199–5204; (*g*) F. Cucinotta, A. Guenet, C. Bizzarri, W. Mróz, C. Botta, B. Milián-Medina, J. Gierschner and L. De Cola, *ChemPlusChem*, 2014, **79**, 45–57; (*h*) E. A. Prasetyanto, P. Manini, A. Napolitano, O. Crescenzi, M. d'Ischia and L. De Cola, *Chem. – Eur. J.*, 2014, **20**, 1597–1601; (*i*) N. S. Kehr, B. Ergün, H. Lülf and L. De Cola, *Adv. Mater.*, 2014, **26**, 3248–3252; (*j*) A. Szarpak-Jankowska, C. Burgess, L. De Cola and J. Huskens, *Chem. – Eur. J.*, 2013, **19**, 14925–14930.

5 (*a*) N. Gfeller, S. Megelski and G. Calzaferri, *J. Phys. Chem. B*, 1999, **103**, 1250–1257; (*b*) H. Lülf, A. Bertucci, D. Septiadi, R. Corradini and L. De Cola, *Chem. – Eur. J.*, 2014, **20**, 10900–10904; (*c*) S. Hashimoto, H. R. Moon and K. B. Yoon, *Microporous Mesoporous Mater.*, 2007, **101**, 10–18; (*d*) Z. Fereshteh, M. R. Loghman-Estarki, R. Shoja Razavi and M. Taheran, *Mater. Sci. Semicond. Process.*, 2013, **16**, 547–553.

6 (*a*) N. Gfeller, S. Megelski and G. Calzaferri, *J. Phys. Chem. B*, 1998, **102**, 2433–2436; (*b*) G. Calzaferri, S. Huber, H. Maas and C. Minkowski, *Angew. Chem., Int. Ed.*, 2003, **42**, 3732–3758; (*c*) A. Z. Ruiz, D. Brühwiler, T. Ban and G. Calzaferri, *Monatsh. Chem.*, 2005, **136**, 77–89; (*d*) A. Devaux, Z. Popović, O. Bossart, L. De Cola, A. Kunzmann and G. Calzaferri, *Microporous Mesoporous Mater.*, 2006, **90**, 69–72; (*e*) I. Cucchi, F. Spano, U. Giovanella, M. Catellani, A. Varesano, G. Calzaferri and C. Botta, *Small*, 2007, **3**, 305–309; (*f*) Z. Popović, M. Otter, G. Calzaferri and L. De Cola, *Angew. Chem., Int. Ed.*, 2007, **46**, 6188–6191; (*g*) S. Suárez, A. Devaux, J. Bañuelos, O. Bossart, A. Kunzmann and G. Calzaferri, *Adv. Funct. Mater.*, 2007, **17**, 2298–2306; (*h*) G. Calzaferri and K. Lutkouskaya, *Photochem. Photobiol. Sci.*, 2008, **7**, 879–910; (*i*) V. Vohra, A. Bolognesi, G. Calzaferri and C. Botta, *Langmuir*, 2010, **26**, 1590–1593; (*j*) G. Calzaferri, *Langmuir*, 2012, **28**, 6216–6231; (*k*) J. M. Beierle, R. Roswanda, P. M. Erne, A. C. Coleman, W. R. Browne and B. L. Feringa, *Part. Part. Syst. Charact.*, 2013, **30**, 273–279.

7 Z. Popović, M. Busby, S. Huber, G. Calzaferri and L. De Cola, *Angew. Chem., Int. Ed.*, 2007, **46**, 8898–8902.

8 (*a*) C. A. Strassert, M. Otter, R. Q. Albuquerque, A. Höne, Y. Vida, B. Maier and L. De Cola, *Angew. Chem., Int. Ed.*,

2009, **48**, 7928–7931; (*b*) J. El-Gindi, K. Benson, L. De Cola, H.-J. Galla and N. Seda Kehr, *Angew. Chem., Int. Ed.*, 2012, **51**, 3716–3720.

9 M. Woerdemann, C. Alpmann, M. Esseling and C. Denz, *Laser Photonics Rev.*, 2013, **7**, 839–854.

10 (*a*) M. Woerdemann, S. Glasener, F. Horner, A. Devaux, L. De Cola and C. Denz, *Adv. Mater.*, 2010, **22**, 4176–4179; (*b*) F. Hoerner, M. Woerdemann, S. Müller, B. Maier and C. Denz, *J. Biophotonics*, 2010, **3**, 468–475.

11 H. Li, Y. Ding, P. Cao, H. Liu and Y. Zheng, *J. Mater. Chem.*, 2012, **22**, 4056–4059.

12 R. Barbey, L. Lavanant, D. Paripovic, N. Schüwer, C. Sugnaux, S. Tugulu and H.-A. Klok, *Chem. Rev.*, 2009, **109**, 5437–5527.

13 M. K. Brinks and A. Studer, *Macromol. Rapid Commun.*, 2009, **30**, 1043–1057.

14 (*a*) A. Mardyukov, Y. Li, A. Dickschat, A. H. Schäfer and A. Studer, *Langmuir*, 2013, **29**, 6369–6376; (*b*) A. Mardyukov and A. Studer, *Macromol. Rapid Commun.*, 2013, **34**, 94–101; (*c*) A. Mardyukov, M. Tesch and A. Studer, *J. Polym. Sci., Part A: Polym. Chem.*, 2014, **52**, 258–266.

15 S. Miele, P. Nesvadba and A. Studer, *Macromolecules*, 2009, **42**, 2419–2427.

16 M. Husseman, E. E. Malmström, M. McNamara, M. Mate, D. Mecerreyes, D. G. Benoit, J. L. Hedrick, P. Mansky, E. Huang, T. P. Russell and C. J. Hawker, *Macromolecules*, 1999, **32**, 1424–1431.

17 K. Min, H. Gao and K. Matyjaszewski, *Macromolecules*, 2007, **40**, 1789–1791.

18 (*a*) C. B. Wagner and A. Studer, *Eur. J. Org. Chem.*, 2010, 5782–5786; (*b*) V. Strehmel, H. Rexhausen and P. Strauch, *Tetrahedron Lett.*, 2008, **49**, 3264–3267; (*c*) V. Strehmel, H. Rexhausen and P. Strauch, *Tetrahedron Lett.*, 2012, **53**, 1587–1591; (*d*) A. Gheorghe, A. Matsuno and O. Reiser, *Adv. Synth. Catal.*, 2006, **348**, 1016–1020.

19 The reaction is performed in the absence of water and O_2, but initial studies showed that DMF/H_2O mixtures as solvents are tolerated as well as the presence of air.

20 K. Hori and S. Matsumoto, *Biochem. Eng. J.*, 2010, **48**, 424–434.

21 A. Z. Ruiz, D. Brühwiler, T. Ban and G. Calzaferri, *Monatsh. Chem.*, 2005, **136**, 77–89.

22 J. P. Magnusson, S. Bersani, S. Salmaso, C. Alexander and P. Caliceti, *Bioconjugate Chem.*, 2010, **21**, 671–678.

23 A. Hashidzume, Y. Zheng, Y. Takashima, H. Yamaguchi and A. Harada, *Macromolecules*, 2013, **46**, 1939–1947.